Environmental Science & Technology

Article

pubs.acs.org/est

pH Dependence of Structure and Surface Properties of Microbial EPS

Ling-Ling Wang,[†] Long-Fei Wang,[†] Xue-Mei Ren,[§] Xiao-Dong Ye,*[,‡] Wen-Wei Li,[†] Shi-Jie Yuan,[†] Min Sun,[†] Guo-Ping Sheng,[†] Han-Qing Yu,*[,†] and Xiang-Ke Wang[§]

[†]Department of Chemistry, [‡]Department of Chemical Physics, University of Science & Technology of People's Republic of China, [§]Institute of Plasma Physics, Chinese Academy of Sciences, Hefei, 230001, People's Republic of China

ABSTRACT: The flocculation of microorganisms plays a crucial role in bioreactors, and is substantially affected by pH. However, the mechanism for such an effect remains unclear. In this work, with an integrated approach, the pH dependence of structure and surface property of microbial extracellular polymeric substances (EPS), excreted from *Bacillus megaterium* TF10, and accordingly its flocculation is elucidated. From the Fourier transform infrared spectra and acid–base titration test results, the main functional groups and buffering zones in the EPS responsible for the microbial flocculation are indentified. The laser light scattering analysis reveals that the deprotonated or protonated states of these functional groups in EPS result in more dense and compact structure at a lower pH because of hydrophobicity and intermolecular hydrogen bonds. The zeta potential measurements identify the isoelectric point and indicate that the electrostatic repulsion action of EPS is controlled by pH. The highest flocculation efficiency is achieved near the isoelectric point (pH 4.8). These results clearly demonstrate that the EPS structure, surface properties, and accordingly the microbial flocculation are dependent heavily on pH in solution.

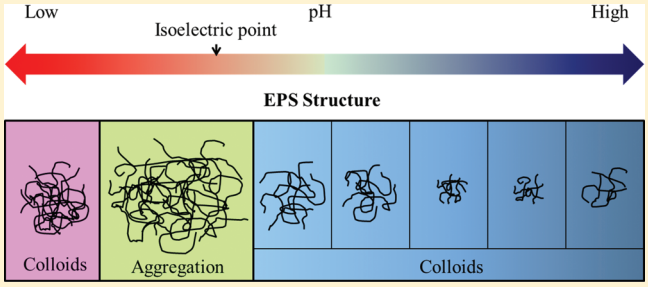

INTRODUCTION

In bioreactors, the flocculation of microbial aggregates plays a crucial role, as it is an important factor determining effluent quality and solid–liquid separation. Such a microbial flocculation is closely related with extracellular polymer substances (EPS) secreted by microorganisms, which have a substantial effect on the properties of microbial aggregates, such as mass transfer, surface characteristics, adsorption ability, stability, and the formation of microbial aggregates.[1−4] The physicochemical properties of EPS are complex and highly related to different functional groups. These groups, such as carboxylic or sulfate groups, generally remain deprotonated at pH above 4.0 due to ionization. In contrast, other EPS functional groups, like thiol-, sulfinic, sulfonic acid and amino groups with p*K* values of 7.0–9.0, are prone to changes in protonation state.[5] The deprotonated or protonated states of different functional groups, which may vary considerably with pH changes, can thus significantly influence the rheological properties, metal binding and organic adsorption capacities, extraction efficiency of EPS as well as their flocculation.[2,6,7]

Microbial EPS production at various pH values has been investigated.[7,8] However, so far little is known about the effect of pH on EPS structure and surface properties, which is closely linked to the EPS physicochemical properties, resulting from the ionization of EPS groups.[8] Some phenomena, such as the flocculation of EPS,[2] and the affinities of EPS to metals and dyes[1] were found to be related with pH. This might be due to the lack of information about the response of EPS structure and surface properties to pH variations. Thus, an insight into the response of EPS structure to pH changes will be beneficial to understanding the correlation between pH and the EPS surface properties and elucidating the mechanisms for the pH dependence of the flocculation of EPS.

In this work, the EPS harvested from a bacterium *Bacillus megaterium* TF10, which was isolated from soil, were selected to evaluate the pH effect on the structure and surface properties of EPS and their relationships with EPS flocculation. Our previous study has shown that this strain has a high EPS-producing capability and their EPS have a flocculation capacity.[9] The chemical elements, functional groups, structural units and linking forms of its key constituents have been identified. It has been reported that the EPS flocculation varies with pH[2] and such a phenomenon might be attributed to the response of EPS structure and surface properties to pH changes. In the present work, we investigated the EPS structure and surface properties at various pH values with a combined use of laser light scattering (LLS), Fourier transform infrared spectra (FTIR), zeta potential (ZP), and acid–base titration techniques. This work elucidates the EPS flocculation mechanisms from the viewpoint of physical chemistry.

MATERIALS AND METHODS

EPS Extraction and Flocculation Assay. EPS were extracted from *Bacillus megaterium* TF10 using EDTA method[6]

Received: October 6, 2011
Revised: December 11, 2011
Accepted: December 15, 2011
Published: December 15, 2011

to remove the divalent cations and the strain was cultured aerobically at 30 °C for 24 h in a Luria−Bertani broth supplied with 10 g/L peptone, 5 g/L yeast extract and 10 g/L NaCl. The crude EPS were concentrated and washed repeatedly with deionized water by using ultrafiltration device with 10 000-NMWL (Nominal Molecular Weight Limit) polyethersulfone ultrafiltration membrane (Millipore Corporation, U.S.) to remove the ions and small molecules, followed by lyophilization. For storage, the obtained powdered EPS were placed in a desiccator at room temperatures and fresh solutions were prepared just before every experiment. The flocculation of EPS at different pHs in a range of 4.0 and 9.0 was determined by measuring the turbidity of a kaolin suspension in a 100-mL beaker according to Yuan et al.[9]

EPS were dissolved in deionized degassed water with an electrical conductivity less than 0.5 μS/cm to a concentration of 1.2 g/L, and then the EPS solution was added into different pH buffers with a volume ratio of 1:1. The buffers were prepared as follows:[10] KCl-HCl for pH 1.3; glycine-HCl for pH 2.5 and 3.6 buffers, with NaCl added to adjust the ionic strength; sodium acetate-acetic acid for pH 4.2−5.6; Na_2HPO_4−NaH_2PO_4 for pH 5.7−7.8; glycine-NaOH for pH 9.2 with NaCl added to adjust the ionic strength; and Na_2HPO_4−NaOH for pH 10.5. All of the buffers were filtered through 0.2-μm filter prior to use. The EPS solutions at different pH values were kept at a concentration of 0.6 g/L and ionic strength of 0.1 M to make sure that the effect of ionic strength is of the same level.

Zeta potential (ZP) was measured at 25 °C using a Nanosizer ZS instrument equipped with backscattering detection at 173° (Malvern Instruments Co., UK). The samples were carefully filled into Zeta potential folded capillary cells (DTS1060) to avoid air bubble formation. Each sample was measured at least 6 times and evaluated by Zeta Quality Report to ensure validity.

FTIR Spectroscopy Analysis. FTIR of samples was recorded with a VERTEX 70 FTIR (Bruker Co., Germany) to determine complexation and dissociation of protons on functional groups. EPS samples were dissolved in deionized water to a concentration of 10 mg/mL. The pH values of three samples were adjusted to approximately 1.3, 7.0, and 10.0, respectively, using 0.2 M HCl or NaOH solution. Then, the prepared samples were lyophilized and mixed into FTIR grade KBr powder. For the purified lyophilized EPS, the samples were directly mixed into KBr powder to test.

Acid−Base Titration. To determine the proton binding sites on EPS surface, acid−base titration was conducted using an automated titrator (DL50 Mettler-Toledo) at 25 °C. EPS of 50 mg were dissolved in 40 mL deionized water and the EPS solution was adjusted to pH 3.0 with 0.2 M HCl. During titration, the EPS solution was continually stirred and sparged with nitrogen to avoid the formation of carbonate ions arise from atmospheric CO_2 dissolution. After 20-min stirring, the EPS solution was automatically titrated using 0.19723 M NaOH calibrated by potassium hydrogen phthalate programmed in incremental monotonic mode with a dosing unit of 5 μL. 40 mL deionized water, whose pH was previously adjusted to pH 3.0 with 0.2 M HCl, was used as control. The obtained titration curves were analyzed with the PROTOFIT 2.1 software.[11]

For titration of EPS, the proton mass balance can be written as follows:

$$\Delta n_{H^+,\mathrm{total},i} = \Delta n_{H^+,\mathrm{wat},i} + \Delta n_{H^+,\mathrm{EPS},i} \quad (1)$$

where Δn_{H^+} refers to the amount of proton added to the system as a whole (total), water, and EPS from the beginning of the titration to step i. The function of Q_{tot} (the total number of protons exchanged with the system, normalized to EPS mass) and derivative function Q^*_{tot} are estimated from the raw titration data:

$$Q_{\mathrm{tot}}(i) = \frac{\Delta n_{H^+,\mathrm{total},i}}{M_{\mathrm{EPS}}} \quad (2)$$

$$Q^*_{\mathrm{tot}}(i) = \frac{dQ_{tot(i)}}{dpH} \quad (3)$$

where M_{EPS} is the mass of EPS. Since it is more convenient to visually compare positive values, the derivative is converted to a positive value.

In a ProtoFit simulation mode, a titration will be simulated with the predictions of a given model, i.e., model-derived $F_{tot}(i)$ and derivative functions $F^*_{tot}(i)$:

$$F_{\mathrm{tot}}(\mathrm{i}) = \frac{\Delta n_{H^+,\mathrm{total,i(p)}}}{M_{\mathrm{EPS}}} \quad (4)$$

$$F^*_{\mathrm{tot}}(i) = \frac{dF_{\mathrm{tot}(i)}}{d\mathrm{pH}} \quad (5)$$

where $\Delta n_{H^+,\ \mathrm{total},\ i(p)}$ is a predicted value obtained from the titration simulation. Model parameters, e.g., equilibrium constants and surface site concentrations, could be optimized with ProtoFit by minimizing the sum of squares between Q^*_{tot} and F^*_{tot}.

LLS Measurements. LLS measurements were conducted on an ALV/DLS/SLS-5022F spectrometer equipped with a multi-τ digital time correlator (ALV5000), and a cylindrical 22 mW UNIPHASE He−Ne laser (λ_0 = 632.8 nm) as the light source. For the LLS measurements, each EPS solution was clarified by a 0.45 μm hydrophilic PTFE (Millipore Millex-LCR) filter into a dust-free vial and carried out at 25.0 ± 0.1 °C.

In static LLS, the angular dependence of the excess Rayleigh ratio (R_{ex}) was measured. the R_{ex} is related to the weight-averaged molecular weight (M_w), the z-average root-mean-square radius of gyration $\langle R_g^2\rangle_z^{1/2}$ (or simply as $\langle R_g\rangle$) as follows: [12,13]

$$\frac{KC}{R_{\mathrm{ex}}} \approx \frac{1}{M_{\mathrm{w}}}\left(1 + \frac{1}{3}\langle R_{\mathrm{g}}^2\rangle_z q^2\right) + 2A_2C \quad (6)$$

where $K = 4\pi^2n^2(\mathrm{d}n/\mathrm{d}C)^2/(N_A\lambda_0^4)$ with n, dn/dC, N_A, and λ_0 being the solvent refractive index, the specific refractive index increment, Avogadro's number, and the wavelength of light in vacuum, respectively. The $q = (4\pi n/\lambda_0)\sin(\theta/2)$ with θ being the scattering angle. To evaluate the EPS colloid inner concentration (C^*) in solution, we calculate C^* (also known as overlap concentration) from the values of M_w and $\langle R_g\rangle$: [14−16]

$$C^* = \frac{3M_{\mathrm{w}}}{4\pi N_{\mathrm{A}}\left\langle R_{\mathrm{g}}\right\rangle^3} \quad (7)$$

We define an index V_R to determine the volume ratio for EPS colloids occupied in solution as follows:

$$V_R = \frac{V_{EPS}}{V_{solution}} = \frac{m_{EPS}/C^*}{V_{solution}} = \frac{m_{EPS}/V_{solution}}{C^*} = \frac{C}{C^*} \quad (8)$$

Thus, the EPS are defined as colloids at $V_R < 1$, but as network at $V_R \geq 1$.

In addition, the geometrical specific surface area (GSSA) is determined by the following:

$$GSSA = \frac{1}{m_{colloid}} \times 4\pi \left\langle R_g \right\rangle^2 = \frac{1}{M_{w,app}/N_A} \times 4\pi \left\langle R_g \right\rangle^2 = \frac{4\pi N_A \left\langle R_g \right\rangle^2}{M_{w,app}} \quad (9)$$

where $m_{colloid}$ is the mass of individual EPS colloid, N_A, $M_{w,app}$ and $\langle R_g \rangle$ are the Avogadro's number, apparent weight-average molar mass, and z-average root-mean-square radius of gyration of EPS colloid, respectively.

In dynamic LLS, the precisely measured intensity−intensity time correlation function $G^{(2)}(q, \tau)$ was measured in the self-beating mode. The Laplace inversion of $G^{(2)}(q, \tau)$ led to a line width distribution $G(\Gamma)$. For a diffusive relaxation, Γ is directly related to the translational diffusion coefficient D. Further, D can be converted to the hydrodynamic radius $\langle R_h \rangle$ by using the Stokes−Einstein equation.[17]

RESULTS

Flocculation and Isoelectric Point of EPS. The effects of the initial solution pH and EPS concentration on the flocculating efficiency of EPS are shown in Figure 1. The curves were double-humped and the highest flocculating efficiency was achieved at pH ≈ 5.0. A higher or lower pH reduced their flocculating efficiency, and no prominent self-flocculation of EPS was observed at pH < 4.0 or pH > 9.0. Figure 2 shows that EPS themselves had a pH-dependent flocculation. A significant turbidity was observed at pH 2.5−4.8, while a clear EPS solution was found at pH 1.3 and pH 5.7−10.5. These three distinct regions are designated as Regions 1, 2, and 3.

A ZP plot of EPS solutions versus pH is also shown in Figure 2. The point where the plot passes through ZP of zero is called the isoelectric point, and such a point was found at pH ≈ 4.8 in this case. The ZPs of EPS solutions at pH 1.3, 2.5, and 3.6 were 15.61 ± 0.99, 16.62 ± 0.63, and 16.06 ± 1.33 mV, respectively, without a significant difference. However, different self-flocculation behaviors were found at the three pH values. The turbidity of EPS solution increased from pH 1.3 to 3.6. The ZP value rapidly decreased from pH 4.2 and reached the isoelectric point at pH 4.8. After that, the ZP value decreased with the increasing pH and gradually became stable at pH 7.0−9.2, followed by a slightly more negative value at pH 10.5.

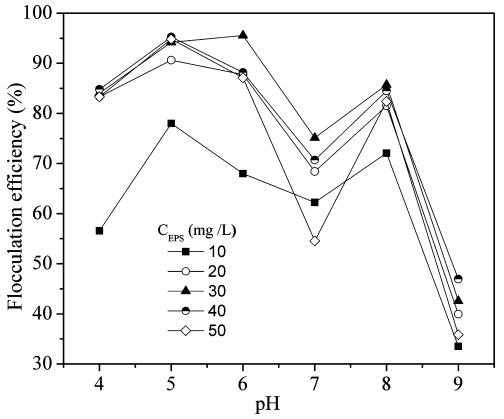

Figure 1. Effect of pH on the flocculating efficiency of EPS solution with kaolin (4 g/L) at $CaCl_2$ of 5.6 mmol/L.

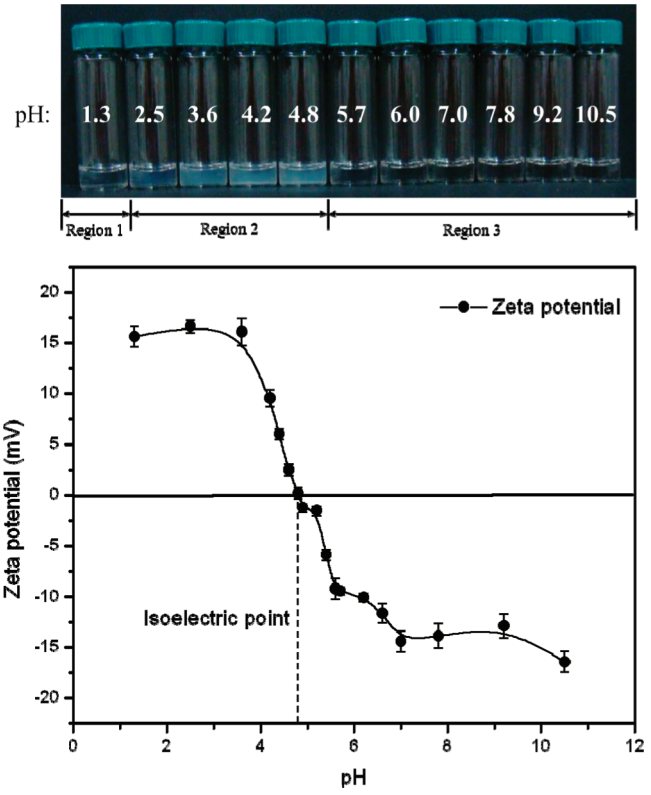

Figure 2. Flocculation behaviors (above, clear solution in Regions 1 and 3, flocs in Region 2) and ZPs (below) of EPS solution of 0.6 g/L at different pHs.

FTIR Spectra of EPS. The functional groups of EPS, which are closely related to the specific chemical properties, were identified by FTIR analysis. This can provide more useful information on EPS structure, because many functional groups have similar pK values, which cannot be well differentiated by titration analysis alone. Figure 3A shows the FTIR spectrum of the purified TF10 EPS, in which several transmittance peaks were found to represent main functional groups. The peak at 3413 cm^{-1} corresponded to O−H stretching and the peak at 2925 cm^{-1} was attributable to C−H stretching.[5] Two minor peaks around 2367 cm^{-1} could be assigned to the O−H stretching vibrations in sulfinic and sulfonic acids.[18] Peak at 1649 cm^{-1} was mainly assigned to C═O and C═C stretching in proteins.[9] The band near 1540 cm^{-1} was associated with the N−H bending

dx.doi.org/10.1021/es203540w | Environ. Sci. Technol. 2012, 46, 737−744

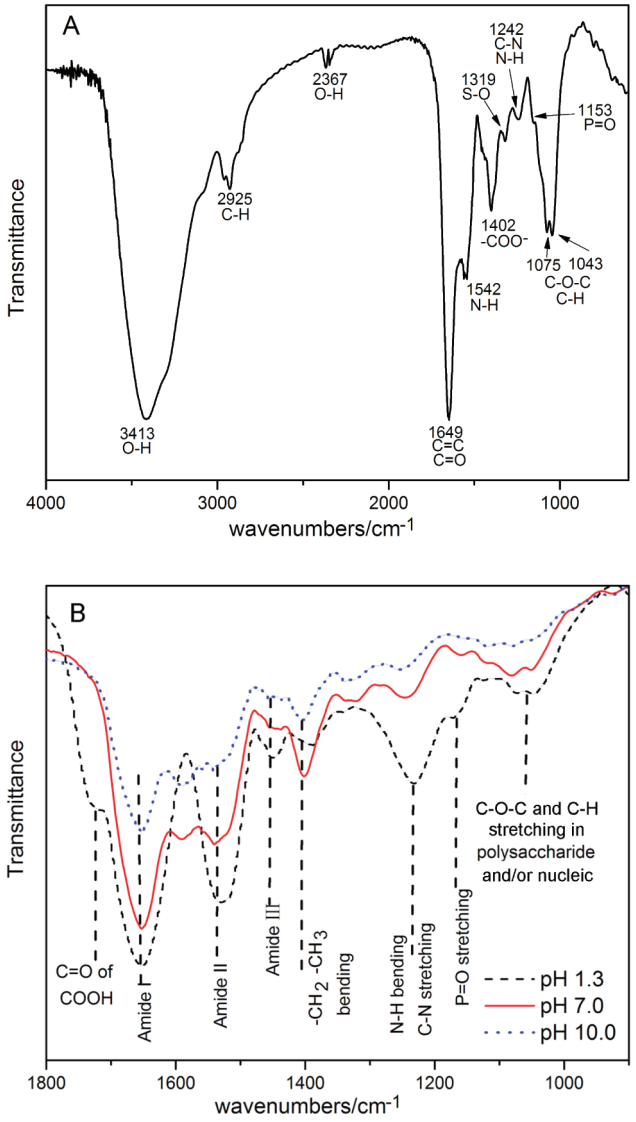

Figure 3. FTIR spectra of the purified EPS (A) and EPS in acidic, neutral, and alkaline solutions (B) [nucleic acids in (B)].

in proteins, while the band near 1402 cm^{-1} was attributed to the symmetric stretching of C═O in COO−.[7,19] A doublet located at 1075 and 1043 cm^{-1} originated from the C−O−C and C−H stretching in polysaccharides and/or nucleic acids. In addition, there were three minor peaks at 1319, 1242, and 1153 cm^{-1}, which were attributed to S−O stretching, N−H bending and C−N stretching vibrations, P═O stretching, respectively.[18]

Figure 3B shows the FTIR spectra of EPS samples under acidic, neutral, and alkaline conditions. The characteristic peaks of EPS were mainly extracted from the region of 1800 cm^{-1} and 900 cm^{-1}.[20] For the EPS in acidic solution, a small peak at 1714 cm^{-1} was observed, which corresponded to C═O stretching of protonated −COOH groups.[7] With an increase in pH, the shoulder peak disappeared due to the continuous dissociation of −COOH groups. Additionally, the peak intensity in the range of 1275−1200 cm^{-1} reflected the extent of H-bonds, and a lower intensity at a higher pH is in agreement with the deprotonation of H-bonds.[21]

Amides I (1600−1700 cm^{-1}) and II (1500−1600 cm^{-1}) regions could be used to interpret the information on the secondary structure of proteins. The proteins changed from a helical conformation (bands between 1660 and 1650 cm^{-1}) at a lower pH to an unordered random coil (band between 1650 and 1640 cm^{-1}) at a higher pH.[7,22] In addition, the intensities of peaks at 1654 cm^{-1} (C═O), 1529 cm^{-1} and 1234−1250 cm^{-1} considerably decreased with the increasing pH, arising from the destruction of amide groups in proteins.

Acid−Base Titration Curves of EPS. The typical acid−base titration curves of EPS and the control are shown in Figure 4A.

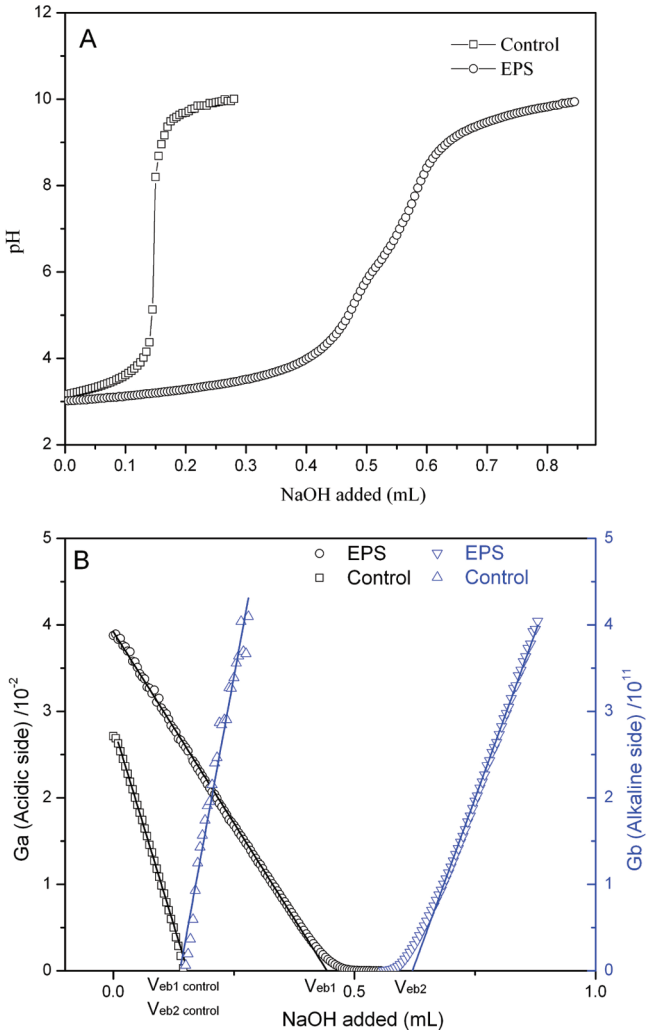

Figure 4. Acid−base titration curves for the EPS solution and the control (A) and Gran plots for titration of EPS and control (B), $G_a = 10^{-pH}(V_0 + V)$ for the acidic side and $G_b = 10^{pH}(V_0 + V)$ for the alkaline side. V_0 is the initial volume of sample, and V is the volume of added NaOH, V_{eb1} and V_{eb2} are the points where G_a and G_b become 0, respectively.

A significant titration jump was observed for the control. This is a typical phenomenon that a strong acid (HCl) is titrated with a strong base (i.e., NaOH). The EPS, however, had a gentler titration curve.

The S-shaped titration curves were further transferred into two straight lines, which were disconnected at the end points (Figure 4B) using a mathematical method proposed by Gran.[23] For heterogeneous materials like EPS, the sorption surface can be regarded as a complex contribution of acidic sites.[24] It is assumed that no other acids dissociate in the first straight line

dx.doi.org/10.1021/es203540w | Environ. Sci. Technol. 2012, 46, 737−744

part of the titration plot and added increments of base cause a linear decrease in $[H^+]$. For the control, the $V_{eb1\ control}$ and $V_{eb2\ control}$ were of almost the same level, resulting from that there was no buffering capacity in strong acid or base systems. However, a distinct difference between V_{eb1} and V_{eb2} was observed for the EPS titration. Initially, the added hydroxyl reacted with extra H^+ in solution, then reacted with the EPS functional groups on the sample surface, and finally resulted in the sharp increase in total pH.[25]

Since microbial surface is complex and the charges on the surface are not concentrated in a single plane, the electrostatic surface complexation model used for mineral surfaces is inappropriate to describe the titration. Instead, a nonelectrostatic model (NEM) with four discrete sites is used to simulate our results.[11,26,27] From the titration data, the nonelectrostatic model with four discrete sites provided the best fit to Q^*_{tot} (Figure 5). The pK values, site densities (mmol kg^{-1}_{dw}) and

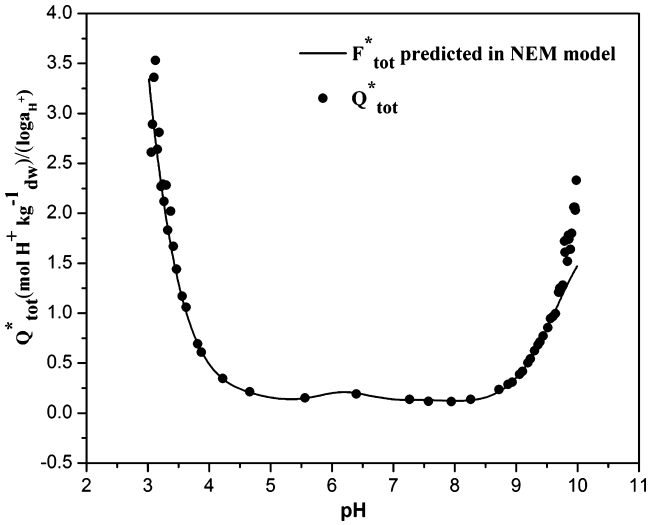

Figure 5. Q^*_{tot} for TF10 EPS and F^*_{tot} (solid line) predicted in the NEM model.

corresponding functional groups of EPS are summarized in Table 1. According to the FTIR spectra, the first pK was

Table 1. Titration Results for TF10 EPS Calculated with PROTOFIT

	pK_1	pK_2	pK_3	pK_4
pK_a value	2.44	6.36	7.57	10.16
site density (mmol kg^{-1}_{dw})	1698	138	166	1445
functional group	carboxylic acids	phosphoric groups	sulfinic acid, sulfonic acid or thiols	thiols, amino

attributed to the carboxyl groups.[25] The pK_2 and pK_3 were at pH 6.36 and pH 7.57, which might be attributed to the phosphoric, thiols, sulfinic and/or sulfonic acid groups that exist in the form of bioorganic molecules in EPS, e.g., proteins.[28] The pK_4 appeared at pH 10.16 and this buffering capacity are usually attributed to amino groups, but thiol with a wide range of pK values may also be involved.[25] For the four sites, the binding site densities were estimated to be 1698, 138, 166, and 1445 mmol kg^{-1}_{dw}, respectively.

Structure of EPS at Different pHs. The structure of EPS at various pHs were determined with the LLS measurement data shown in Table 2. It was found that the EPS in these solutions were in the form of colloids or EPS solutions were in dilute regime, because the V_R values of all the EPS samples were less than 1.0. However, the sizes of EPS, including $\langle R_g \rangle$ and $\langle R_h \rangle$ of EPS colloids, were of nearly the same level in acidic and neutral solutions, and became smaller in alkaline solution. It is worth noting that the ratio $\rho = \langle R_g \rangle / \langle R_h \rangle$ is a parameter directly related to the chain architecture. Here, all of the ρ values of the EPS colloids were less than 1.5, indicating that the shapes of these EPS colloids were random coil with incompletely extending chains. A slightly higher value of ρ was found in alkaline solution, which was responsible for a little extended chain structure of EPS under alkaline conditions.

To provide more information about the EPS colloids, the apparent weight-average molar mass $M_{w,app}$, colloid inner concentration C^*, and GSSA were calculated (Table 2). The decrease in $M_{w,app}$ of the EPS colloid with the increasing pH was significant and the inner concentration C^* at pH 1.3 and 6.0 were 12.6 and 5.08 g/L, respectively, which were substantially higher than those in neutral and alkaline solutions. There was a more compressed and dense structure of EPS in acidic solution. On the contrary, the GSSA was found to increase with pH.

DISCUSSION

Evolution of EPS Structure and Surface Properties Affected by pH. EPS are essentially a mixture of biomolecules, which can be treated as "soft matter"[29] and their structure can be affected by surroundings.[8] Meanwhile, as amphoteric substances, the neutral, positively-, and negatively-charged surface species all coexist in EPS colloidal form. Thus, their balance in EPS colloid structure might be easily destroyed and restructured when pH changes.

In Regions 1 and 3, the LLS analysis reveals a significant change of EPS structure with pH variation (Table 2). The changes of EPS molecular configurations with pH were also observed by others.[30] The observation that EPS tend to have more dense and compact structure in Region 1 agrees with the small-angle X-ray scattering (SAXS) result reported by Dogsa et al.[8] They found that the EPS from a marine bacterium demonstrated a structure of network of randomly coiled polymeric chains, and that dense domains increased in average size from 19 nm at pH 11.0 to 52 nm at pH 0.7. Considering that the EPS concentration used in their study was 0.4% w/v (approximately 4 g/L), it was reasonable that their EPS had a relatively homogeneous network structure at a higher pH and became deswollen at a lower pH. In comparison, the EPS concentration in our work is 0.6 g/L, thus, the EPS retain their colloid structure in clear solution.

The corresponding functional groups and their pK values, site densities in EPS are determined by acid−base titration. These results should be consistent with the FTIR results, which provide the group information and relative abundances. Also, the FTIR results demonstrate that there are more carboxylic, destruction of amide groups and unordered random coil conformation at a higher pH (Region 3). Thus more hydrophilic and ion groups at a higher pH need to be stabilized with a larger total interfacial area, which generally results in smaller particles.[31] This explains the dispersing, lower density, smaller size structure, and higher GSSA of EPS colloids at a higher pH (Table 2), as illustrated in Figure 6. These differences were

Table 2. LLS Data Summary for EPS Solution at Different pHs

pH	C (g/L)	$\langle R_h \rangle$ (nm)	$\langle R_g \rangle$ (nm)	ρ	$M_{w,app}$ (g/mol)	C* (g/L)	V_R	GSSA (m^2/g)
1.3	0.6	83	96	1.16	2.81×10^7	12.6	0.05	2.48×10^3
6.0	0.6	82	96	1.18	1.13×10^7	5.08	0.12	6.18×10^3
7.0	0.6	80	92	1.15	4.35×10^6	2.22	0.27	1.48×10^4
7.8	0.6	47	58	1.25	1.60×10^6	3.25	0.18	1.61×10^4
9.2	0.6	45	62	1.36	1.25×10^6	2.08	0.29	2.34×10^4
10.5	0.6	66	80	1.22	1.24×10^6	0.96	0.63	3.90×10^4

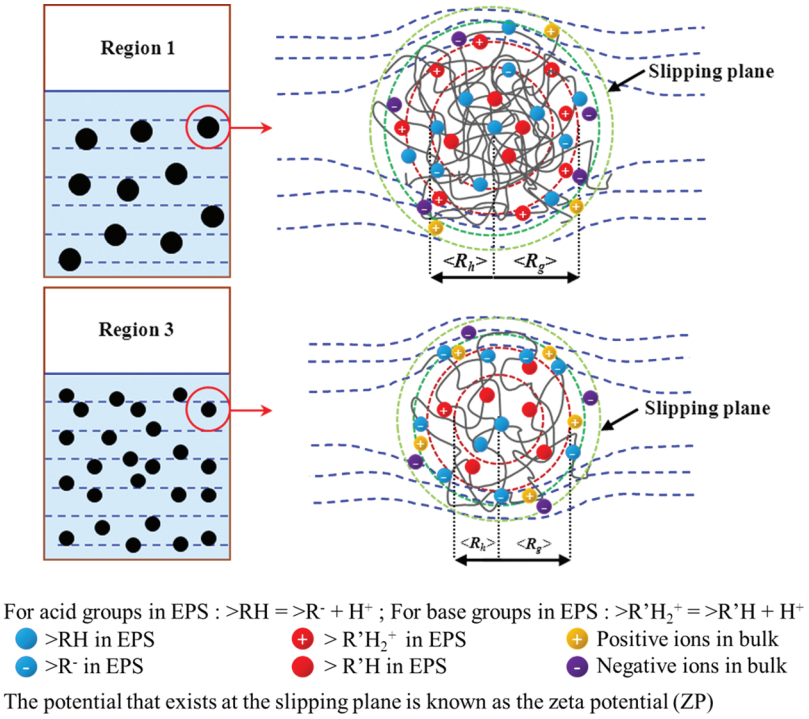

Figure 6. Schematic illustration for the structure and surface properties of EPS colloids in Regions 1 (EPS colloids are positively charged) and 3 (EPS colloids are negatively charged).

confirmed by the ZPs (Figure 2) and GSSA (Table 2) results. However, more exposed EPS groups release more binding H^+ into bulk, causing a gentler titration curve (Figure 4A) and lower slope of Gran plot (Figure 4B).

However, the ZPs of EPS seem to be less related with the flocculation performance and conformation of EPS. Such a discrepancy was also found in previous studies. The ZPs seemed to be not correlated with the relative hydrophobicity[32] and the trends of deposition efficiency for soluble or bound EPS did not totally correspond to the trends of ZPs.[33] This might be attributed to the EPS structure rearrangements and the charged surface species, counterions alteration with pH variation (Figure 6).

Intra- and Inter-Colloid Interactions of EPS at Different pHs. The intra- and inter-colloid interactions are complicated and subtle due to the complex EPS compositions. The polysaccharides or proteins can form gel or aggregation, due to pH changes.[8] Thus, the polysaccharides and proteins in EPS are supposed to be involved in the intra- and inter-colloid interactions due to their titratable groups.

In Region 1, the dominating force may be the electrostatic repulse due to the high positive charged EPS (ZP result) and the hydrophobicity, intermolecular hydrogen bonds (FTIR result) promotes the larger, compressed, and denser structure of EPS in solution. EPS are known as typical amphoteric substances and confirmed by the titration data, for which the electrostatic repulsion and ionic hydration are minimal at the isoelectric point.[34] Therefore, the attraction force prevails in Region 2 and leads to flocculation of EPS. It is worth noting that the isoelectric point is not in the center of Region 2. If there are no other reasons for the flocculation besides hydrophobicity, it will be centered. However, our FTIR analysis shows that intra- and inter- colloid H-bonds were formed at a lower pH. In this case, EPS colloids became destabilized and formed aggregates. In Region 3, the intra- and inter-colloid interactions become weak due to the electrostatic repulsion, which results from more EPS negative groups. This also leads to the releasing of chains, swelling and lower density structure of EPS colloids at higher pH in LLS results. However, Regions 1−3 depend on the EPS compositions with their own properties, and might be different for different microbial EPS production.

Flocculation of EPS at Different pHs. In our previous work, it was found that EPS of *B. megaterium* TF10 exhibit a high flocculation at pH 7.0.[9] In the present work, the optimal pH for the flocculation of EPS of *B. megaterium* TF10 was around 5.0, which is close to the isoelectric point of EPS (~pH 4.8). The flocculation of EPS is highly related to the structure and surface properties of EPS.

As shown in Figure 1, the flocculation is double-humped. The second hump may be related to the pK_3 (7.57) of sulfinic acid, sulfonic acid or thiols. These groups are more negative at pH 8.0, and provided more sites for Ca^{2+} bridging in flocculation assay. A little higher C* value at pH 7.8 than at pH 7.0 or 9.2 (Table 2) suggests that the EPS structure rearrangements lead to nonmonotonic interaction in Region 3. Therefore, the EPS flocculation ability may be attributed to the complex interaction variations of EPS with pH.

Significance of This Work. The mechanism for the pH-dependence of microbial EPS surface properties and flocculation ability has not been elucidated. In this work, with a combined use of the LLS, FTIR, Zeta potential, and acid–base titration techniques, the functional groups in EPS are identified as the main contributor, and their complex and subtle intra/inter-actions are recognized to be responsible for the pH dependence of flocculation. As a result, the structure and surface properties of EPS from *Bacillus megaterium* TF10, which have a close relationship with its flocculation, are found to be pH dependent. Our work gives insight into the flocculation mechanisms of microbial EPS and provides useful information on the alteration of EPS properties by pH. For instance, our conclusion that EPS can easily release chains at a higher pH, could be used to explain an observed phenomenon: microbial EPS can be extracted more readily by using the NaOH method than the other extraction techniques.[6]

AUTHOR INFORMATION

Corresponding Author

*Fax: +86 551-3606742; e-mail: xdye@ustc.edu.cn (X.-D.Y); Fax: +86 551-3607592; E-mail: hqyu@ustc.edu.cn (H.-Q.Y.).

ACKNOWLEDGMENTS

We thank the Natural Science Foundation of China (50738006 and 50978243) and the Fundamental Research Funds for the Central Universities (WK206019007) for the partial support of this work.

NOMENCLATURE

C	EPS concentration
C^*	inner or overlap concentration
FTIR	Fourier transform infrared spectra
F_{tot} (i)	model-derived total number of protons exchanged with the system, normalized to EPS mass, in a ProtoFit simulation
F^*_{tot} (i)	derivative function of F_{tot} (i)
GSSA	geometrical specific surface area
LLS	laser light scattering
$M_{w,app}$	apparent weight-average molar mass
NEM	nonelectrostatic model
NMWL	nominal molecular weight limit
pH	the negative logarithm of the molar concentration of dissolved hydronium ion
pK	The negative logarithm of the dissociation constant K
Q_{tot} (i)	the total number of protons exchanged with the system, normalized to EPS mass
Q^*_{tot} (i)	derivative function of Q_{tot} (i)
$\langle R_g \rangle$	z-average root-mean-square radius of gyration
$\langle R_h \rangle$	mean hydrodynamic radius
SAXS	small-angle X-ray scattering
V_R	volume ratio of EPS colloids containing solvent occupied in solution
ZP	zeta potential
ρ	ratio of $\langle R_g \rangle$ to $\langle R_h \rangle$

REFERENCES

(1) Sheng, G. P.; Yu, H. Q.; Li, X. Y. Extracellular polymeric substances (EPS) of microbial aggregates in biological wastewater treatment systems: A review. *Biotechnol. Adv.* **2010**, *28*, 882–894.

(2) Salehizadeh, H.; Shojaosadati, S. A. Extracellular biopolymeric flocculants—Recent trends and biotechnological importance. *Biotechnol. Adv.* **2001**, *19*, 371–385.

(3) Brown, M. J.; Lester, J. N. Metal removal in activated sludge: the role of bacterial extracellular polymers. *Water Res.* **1979**, *13*, 817–837.

(4) Harris, R. H.; Mitchell, R. The role of polymers in microbial aggregation. *Annu. Rev. Microbiol.* **1973**, *27*, 27–50.

(5) Braissant, O.; Decho, A. W.; Dupraz, C.; Glunk, C.; Przekop, K. M.; Visscher, P. T. Exopolymeric substances of sulfate-reducing bacteria: Interactions with calcium at alkaline pH and implication for formation of carbonate minerals. *Geobiology* **2007**, *5*, 401–411.

(6) Sheng, G. P.; Yu, H. Q.; Yu, Z. Extraction of extracellular polymeric substances from the photosynthetic bacterium *Rhodopseudomonas acidophila*. *Appl. Microbiol. Biotechnol.* **2005**, *67*, 125–130.

(7) Omoike, A.; Chorover, J. Spectroscopic study of extracellular polymeric substances from *Bacillus subtilis*: Aqueous chemistry and adsorption effects. *Biomacromolecules* **2004**, *5*, 1219–1230.

(8) Dogsa, I.; Kriechbaum, M.; Stopar, D.; Laggner, P. Structure of bacterial extracellular polymeric substances at different pH values as determined by SAXS. *Biophys. J.* **2005**, *89*, 2711–2720.

(9) Yuan, S. J.; Sun, M.; Sheng, G. P.; Li, Y.; Li, W. W.; Yao, R. S.; Yu, H. Q. Identification of key constituents and structure of the extracellular polymeric substances excreted by *Bacillus megaterium* TF10 for their flocculation capacity. *Environ. Sci. Technol.* **2011**, *45*, 1152–1157.

(10) Rex, M. C. D.; Daphne, C. E.; William, H. E.; Kenneth, M. J. *Data for Biochemical Research*; Clarendon Press: Oxford, 1986.

(11) Turner, B. F.; Fein, J. B. Protofit: A program for determining surface protonation constants from titration data. *Comput. Geosci.* **2006**, *32*, 1344–1356.

(12) Zimm, B. The scattering of light and the radial distribution function of high polymer solutions. *J. Chem. Phys.* **1948**, *16*, 1093–1099.

(13) Tao, Y. Z.; Yan, F.; Zhang, L. Fractionation and characterization of a protein-polysaccharide complex from Pleurotus tuberregium sclerotia. *J. Polym. Sci. Part B-Polym. Phys* **2007**, *45*, 2546–2554.

(14) de Gennes, P. G. *Scaling Concepts in Polymer Physics*; Cornell University Press: Ithaca, NY, 1979.

(15) Burchard, W. Solution properties of branched macromolecules. *Adv. Polym. Sci.* **1999**, *143*, 113–194.

(16) Teraoka, I. *Polymer Solutions*; John Wiley & Sons: New York, 2002.

(17) Chu, B. *Laser Light Scattering*; Academic Press: New York, 1991.

(18) Coates, J. *Interpretation of Infrared Spectra, A Practical Approach*; John Wiley and Sons Ltd: Chichester, 2000.

(19) Nara, M.; Tasumi, M.; Tanokura, M.; Hiraoki, T.; Yazawa, M.; Tsutsumi, A. Infrared studies of interaction between metal ions and Ca^{2+} binding proteins-marker bands for identifying the types of coordination of the side-chain COO^- groups to metal ions in pike parvalbumin (pI = 4.10). *FEBS Lett.* **1994**, *349*, 84–88.

(20) Schmitt, J.; Flemming, H. C. FTIR-spectroscopy in microbial and material analysis. *Int. Biodeterior. Biodegrad.* **1998**, *41*, 1–11.

(21) Casal, H. L.; Mantsch, H. H. Polymorphic phase behaviour of phospholipid membranes studied by infrared spectroscopy. *Biochim. Biophys. Acta* **1984**, *779*, 381–401.

(22) Buijs, J.; Norde, W.; Lichtenbelt, J. W. T. Changes in the secondary structure of adsorbed IgG and F(ab')$_2$ studied by FTIR spectroscopy. *Langmuir* **1996**, *12*, 1605–1613.

(23) Gran, G. Determination of the equivalence point in potentiometric titrations. *Analyst* **1952**, *77*, 661–671.

(24) Naja, G.; Mustin, C.; Volesky, B.; Berthelin, J. A high-resolution titrator: A new approach to studying binding sites of microbial biosorbents. *Water Res.* **2005**, *39*, 579–588.

(25) Stumm, W.; Morgan, J. J. *Aquatic Chemistry-Chemical Equilibria and Rates in Natural Waters*; John Wiley&Sons: New York, 1996.

(26) Ojeda, J. J.; Romero-Gonzalez, M. E.; Bachmann, R. T.; Edyvean, R. G. J.; Banwart, S. A. Characterization of the cell surface and cell wall chemistry of drinking water bacteria by combining XPS, FTIR spectroscopy, modeling, and potentiometric titrations. *Langmuir* **2008**, *24*, 4032−4040.
(27) Borrok, D.; Turner, B. F.; Fein, A. B. A universal surface complexation framework for modeling proton binding onto bacterial surfaces in geologic settings. *Am. J. Sci.* **2005**, *305*, 826−853.
(28) Sokolov, I.; Smith, D. S.; Henderson, G. S.; Gorby, Y. A.; Ferris, F. G. Cell surface electrochemical heterogeneity of the Fe(III)-reducing bacteria *Shewanella putrefaciens*. *Environ. Sci. Technol.* **2001**, *35*, 341−347.
(29) de Gennes, P. G. Soft Matter. *Science* **1992**, *256*, 495−497.
(30) Sheng, G. P.; Yu, H. Q. Characterization of extracellular polymeric substances of aerobic and anaerobic sludge using three-dimensional excitation and emission matrix fluorescence spectroscopy. *Water Res.* **2006**, *40*, 1233−1239.
(31) Zhang, G.; Li, X.; Jiang, M.; Wu, C. Model system for surfactant-free emulsion copolymerization of hydrophobic and hydrophilic monomers in aqueous solution. *Langmuir* **2000**, *16*, 9205−9207.
(32) Geng, Z. H; Hall, E. R. A comparative study of fouling-related properties of sludge from conventional and membrane enhanced biological phosphorus removal processes. *Water Res.* **2007**, *41*, 4329−4338.
(33) Zhu, P. T.; Long, G. Y.; Ni, J. R.; Tong, M. P. Deposition kinetics of extracellular polymeric substances (EPS) on silica in monovalent and divalent salts. *Environ. Sci. Technol.* **2009**, *43*, 5699−5704.
(34) Damodaran, S. *Food Proteins and Their Applications*; Marcel Dekker: New York, 1997.